Investigation of current injection in β-FeSi$_2$/Si double-heterostructures light-emitting diodes by molecular beam epitaxy

Y. Ugajin, T. Sunohara and T. Suemasu

Institute of Applied Physics, University of Tsukuba, 1-1-1 Tennohdai, Tsukuba, Ibaraki 305-8573, Japan

The p-Si/p-β-FeSi$_2$/p-Si/n-Si light-emitting diode (LED) was fabricated by molecular beam epitaxy (MBE) on Si (111) substrates. Compared to our previous p-Si/p-β-FeSi$_2$/n-Si double-heterostructures (DH) LED, the turn-on voltage in the current-voltage (I-V) characteristics increased by approximately 0.2 V, meaning that defect densities at around the p-n junction was reduced. However, Si-related EL (1.05 eV) became dominant unexpectedly, and thus EL of β-FeSi$_2$ was suppressed accordingly. The origin of the luminescence is considered to be transitions via defect levels (1.05 eV) being due probably to Fe-B complex.

Keywords: β-FeSi$_2$, double-heterostructures, luminescence, *p-n* junction

Corresponding author: Prof. T.Suemasu, Institute of Applied Physics, University of

Tsukuba, Tsukuba, Ibaraki 305-8573, Japan.

TEL(FAX): +81-29-853-5111, Email: suemasu@bk.tsukuba.ac.jp

1. Introduction

Since the demonstration of electroluminescence (EL) from semiconducting iron disilicide (β-FeSi$_2$) precipitates embedded in a Si *p-n* junction by ion beam synthesis (IBS) [1], this material has been attracting remarkable attention. β-FeSi$_2$ can be grown epitaxially on Si substrates, and also has an emission wavelength (~1.5 μm) relevant to optical fiber communication at room temperature (RT). Thus, we think that this material is very promising as light emitters for optical interconnect in future Si integrated circuits. There have been several reports to date on 1.6 μm EL at RT from β-FeSi$_2$ particles embedded in Si *p-n* diodes formed on Si(001) by IBS and by molecular beam epitaxy (MBE) [2-7]. Further efforts have been paid to enhance the luminescence intensity [8,9]. One way to enhance the EL intensity of β-FeSi$_2$ is to embed a β-FeSi$_2$ continuous film in Si as an active region instead of β-FeSi$_2$ particles, and to form Si/β-FeSi$_2$ film/Si (SFS) double heterostructures (DH). Recently, Sunohara *et al*. reported the formation of SFS DH on Si (001) [10]. This has been only one report so far on the formation of SFS DH on Si(001) because a β-FeSi$_2$ epitaxial film grown

on Si(001) exhibits a strong tendency to form islands when annealed at a high temperature to

improve crystalline quality [11]. In contrast, there have been several reports showing that

β-FeSi$_2$ films can be grown on Si(111) even at high temperatures, in spite of the large lattice

mismatch (~5%) between the two materials [12,13]. Chu *et al.* reported EL from SFS DH on

Si(111) [14]. The EL intensity was, however, just comparable to that of Si at RT, indicating

that the EL intensity of β-FeSi$_2$ is weak. They formed the β-FeSi$_2$ film by an rf

magnetron-sputtering technique, and this film was covered with a Si overlayer by chemical

vapor deposition [15]. We have adopted MBE technique to form β-FeSi$_2$ and developed the

formation technique of SFS DH on Si(111) [16]. Very recently 1.6 μm EL was realized at RT

in SFS DH light-emitting diodes (LEDs) on *n*-Si(111) [17]. Undoped β-FeSi$_2$ films grown by

MBE usually exhibit *p*-type conductivity [18,19], and thus the *p-n* junction was formed by an

n-type Si(111) substrate and undoped *p*-type β-FeSi$_2$. However, the turn-on voltage in the

current-voltage (*I-V*) characteristics of the LEDs is typically 0.8 V smaller at RT than that

expected (~1.1 V) [20]. This result suggests that voltages across the *p-n* junction were reduced,

meaning that numerous defects exist around the β-FeSi$_2$/Si p-n heterojunction. We think that these defects are due probably to the lattice mismatch between the two materials, and they prevent carrier injection into β-FeSi$_2$.

In this study, we formed a Si p-n homojunction in LEDs instead of a β-FeSi$_2$/Si p-n heterojunction, and investigated its effect on the I-V characteristics and luminescence properties in SFS DH LEDs.

2. Experimental

The p-Si/p-β-FeSi$_2$/p-Si/n-Si LEDs were fabricated on a 4-μm-thick n-type epitaxial Si (ρ=0.1-1Ω·cm)/Czochralski n^+-Si(111) (ρ=0.004 Ω·cm) substrate. An ion-pumped MBE system equipped with electron-gun evaporation sources for Si and Fe was used. After cleaning the Si(111) substrate at 850°C for 30 min in UHV, and confirming a well-developed 7×7 reflection high-energy electron diffraction (RHEED), approximately 200-nm-thick undoped Si was grown at 450°C by MBE, and annealed at 1000°C for 10 min.

This undoped Si layer was actually p-type with hole concentrations of approximately 2×10^{16} cm^{-3} since B is accumulated [21]. Next, using a 20-nm-thick highly [110]/[101]-oriented β-FeSi$_2$ epitaxial template formed by reactive deposition epitaxy (RDE) at 650°C, undoped p-β-FeSi$_2$ continuous films were grown by MBE at 750°C. The RDE-grown template works as a seed crystal for crystallization of the MBE-grown overlayers [16]. The total thickness of the β-FeSi$_2$ was 90 nm. Next, a 500-nm-thick undoped p-type Si was grown at 500°C and a 200-nm-thick B-doped p^+-Si was subsequently grown by MBE at 700°C. Finally, the wafer was annealed at 800°C in N$_2$ for 14 h [16]. For comparison, sample without the 1000°C-annealed p-Si layer was also prepared. Hereafter, we denote the latter and the former LEDs as samples A and B, respectively.

The crystal quality of the grown layers was characterized by X-ray diffraction (XRD), and the surface morphology was observed by atomic force microscopy (AFM). PL measurements were performed at 77 K with a photoexcitation source at 442 nm, provided by a He-Cd laser. EL spectra were measured at 77 K under 200-Hz pulsed current biasing

with a 50 % duty cycle. Luminescence was dispersed by a 25-cm focal-length grating

monochromator, and detected phase sensitively by a liquid nitrogen cooled InP/InGaAs

photomultiplier (Hamamatsu Photonics R5509-72).

3. Results and discussion

Figures 1(a) and 1(b) show the schematic layered structures of samples A and B,

respectively. The θ-2θ XRD patterns of the samples are shown in Fig. 2. Highly [110]

and/or [101]-oriented β-FeSi$_2$, matching the epitaxial relationship between β-FeSi$_2$ and Si,

was formed in both samples [22]. Weak peaks corresponding to β-FeSi$_2$ (040) and/or (004),

and [100]-oriented β-FeSi$_2$ peaks such as (600) and (800) are observed in sample A;

however, these peaks are much smaller than [110] and/or [101]-oriented peaks. Therefore,

we think that there is no significant difference in crystallinity between samples A and B.

The RHEED patterns taken along [1-10] azimuth of Si after the growth of β-FeSi$_2$ and the

500-nm-thick undoped Si in sample A are shown in Figs. 3(a) and 3(b), respectively.

Similar results were also obtained in sample B. The RHEED pattern was streaky after the

growth of β-FeSi$_2$, as shown in Fig. 3(a); however, the spotty pattern was usually observed

throughout the growth of Si overlayers. The Si overlayer grown on β-FeSi$_2$ has a strong

tendency to form polycrystalline structures with increasing a β-FeSi$_2$ thickness, due

probably to degradation in surface morphology of β-FeSi$_2$ layers. Sunohara *et al*. reported

that in accordance with increasing the β-FeSi$_2$ thickness, RHEED patterns of Si overlayers

grown on β-FeSi$_2$ changed from streaky to spotty, and further to ring [10]. The RMS

roughness of approximately 7 nm obtained after the growth of 90-nm-thick β-FeSi$_2$ may

affect the crystallinity of Si overlayers [16].

Figure 4 shows PL spectra measured at 77 K. The luminescence spectra are almost

the same in both samples. However, we should note that significant difference was observed

in EL spectra as shown in Fig. 5. Figure 5 shows EL spectra measured at 77 K. EL of

β-FeSi$_2$ is dominant in sample A. In contrast, Si-related EL is intense in sample B. The

emission around 1.10 eV is attributed to a transition with the assistance of a transverse

optical (TO) phonon (58 meV) in Si [23]. One of the origins of the emission around 1.05 eV

is due probably to localized traps related to Fe-B complex in the 1000°C-annealed p-Si

layers [24]. Fe and B are considered to be diffused from the β-FeSi$_2$ layer and B

accumulation region at the Si MBE layer/n-Si substrate interface, respectively [21, 25]. The

direction of electrons traversing into β-FeSi$_2$ is different in between EL and PL

measurements. Most of photo-excited electrons and holes are generated in the p-Si capping

layer in PL since a photoexcitation source at 442 nm was used, and they are diffused into

β-FeSi$_2$ from the p-Si capping layer. On the other hand, the electrons are injected into

β-FeSi$_2$ from the n-Si substrate in EL. We therefore think that electron injection into β-FeSi$_2$

is unexpectedly deficient in EL for sample B, because a large number of electrons

recombine with holes via the above-mentioned defects in the p-Si layer.

Figure 6 shows the forward-biased I-V characteristics measured at 77 K and RT.

The turn-on voltage in sample B is increased a little (~0.3 V) by forming a Si p-n junction in

place of a β-FeSi$_2$/Si p-n heterojunction, meaning that defect densities at the p-n junction

were decreased. However, it's far away from the ideal one (~1.1 V). At 77 K, the turn-on

voltage reaches approximately 1.0 V. This result suggests that numerous defects including

Fe-B complex and others still exist around the *p-n* junction. Li *et al.* reported that the LEDs

with high temperature Si buffer layer have shown smaller leakage current than those

without the Si buffer layer [26]. In this work, we fabricated the *p*-Si layer at relatively low

temperature of 450°C. We believe a high-quality Si *p-n* junction improves the electron

injection into β-FeSi$_2$, and thus significant EL enhancement will be obtained.

4. Conclusion

We have fabricated the *p*-Si/*p*-β-FeSi$_2$/*p*-Si/*n*-Si LEDs on Si (111) substrates by MBE,

and investigated carrier injection into β-FeSi$_2$. Compared to DH LEDs using a β-FeSi$_2$/ Si

p-n heterojunction, the turn-on voltage in the *I-V* characteristics was increased by

approximately 0.3 V at RT, meaning that defect densities at the *p-n* junction was decreased.

However, the Si-related EL with the assistance of a TO phonon emission, and via defect

levels being due probably to Fe-B complex in p-type Si was enhanced.

Acknowledgements

References

[1] D. Leong, M. Harry, K. J. Reeson, K. P. Homewood, Nature **387** (1997) 686.

[2] T. Suemasu, Y. Negishi, K. Takakura, F. Hasegawa, Jpn. J. Appl. Phys., Part 2 **39** (2000) L1013.

[3] T. Suemasu, Y. Negishi, K. Takakura, F. Hasegawa, T. Chikyow, Appl. Phys. Lett. **79** (2001) 1804.

[4] M. A. Lourenco, T. M. Butler, A. K. Kewell, R. M. Gwilliam, K. J. Kirkby, K. P. Homewood, Jpn. J. Appl. Phys., Part 1 **40** (2001) 4041.

[5] L. Martinelli, E. Grilli, M. Guzzi, M. G. Grimaldi, Appl. Phys. Lett. **83** (2003) 794.

[6] C. Li, T. Suemasu, F. Hasegawa, J. Appl. Phys. **97** (2005) 043529.

[7] T. Sunohara, C. Li, Y. Ozawa, T. Suemasu, F. Hasegawa, Jpn. J. Appl. Phys., Part 1 **44** (2005) 3951.

[8] Y. Maeda, Y. Terai, M. Itakura, N. Kuwano, Thin Solid Films **461** (2004) 160.

[9] Y. Terai, Y. Maeda, Appl. Phys. Lett. **84** (2004) 903.

[10] T. Sunohara, K. Kobayashi, T. Suemasu, Thin Solid Films **508** (2006) 371.

[11] T. Suemasu, M. Tanaka, T. Fujii, S. Hashimoto, Y. Kumagai, F. Hasegawa, Jpn. J. Appl.

Phys., Part 2 **36** (1997) L1225.

[12] C. Lin, L. Wang, X. Chen, L. F. Chen, L. M. Wang, Jpn. J. Appl. Phys., Part 1 **37**

(1998) 622.

[13] T. Koga, H. Tatsuoka, H. Kuwabara, Appl. Surf. Sci. **169-170** (2001) 310.

[14] S. Chu, T. Hirohada, H. Kan, T. Hiruma, Jpn. J. Appl. Phys., Part 2 **43** (2004) L154.

[15] S. Chu, T. Hirohada, H. Kan, Jpn. J. Appl. Phys., Part 2 **41** (2002) L1200.

[16] M. Takauji, N. Seki, T. Suemasu, F. Hasegawa, M. Ichida, J. Appl. Phys. **96** (2004)

2561.

[17] M. Takauji, C. Li, T. Suemasu, F. Hasegawa, Jpn. J. Appl. Phys., Part 1 **44** (2005)

2483.

[18] N. Hiroi, T. Suemasu, K. Takakura, N. Seki, F. Hasegawa, Jpn. J. Appl. Phys., Part 2 **40**

(2001) L1008.

[19] N.Seki, K.Takakura, T.Suemasu, F.Hasegawa, Materials Science in Semiconductor

Processing **6** (2003) 307.

[20] Y. Ugajin, M. Takauji, T. Suemasu, Thin Solid Films **508** (2006) 376.

[21] H. Kanaya, H. Shigekawa, F. Hasegawa, E. Yamaka, Jpn. J. Appl. Phys., Part 2 **29**

(1990) L195.

[22] J. E. Mahan, V. Le. Thanh, J. Chevrier, I. Berbezier, J. Derrien, and R. G. Long, J. Appl.

Phys. **74** (1993) 1747.

[23] S. Fukatsu, N. Usami, Y. Shiraki, Jpn. J. Appl. Phys., Part 1 **32** (1993) 1502.

[24] T. Miki, Y. Matsui, Y. Teraoka, Y. Ebina, K. Matsubara, K. Kishimoto, J. Appl. Phys. **76**

(1994) 2097.

[25] R. Kuroda, H. Tanoue, Y. Makita, S. Wang, Y. Fukuzawa, N. Otogawa, Y. Nakayama, J.

Appl. Phys. **95** (2004) 4019.

[26] C. Li, H. Lai, S. Chen, T. Suemasu and F. Hasegawa, J. Cryst. Growth **290** (2006) 176.

Figure captions

Fig. 1   Schematic layered structures of samples A (a) and B (b).

Fig. 2 θ-2θ XRD patterns of samples A and B.

Fig. 3   RHEED patterns taken after the growth of (a) β-FeSi$_2$ and (b) undoped p-type Si layers

in sample B.

Fig. 4   PL spectra of samples A and B measured at 77 K.

Fig. 5   EL spectra of LEDs, made from samples A and B, measured at 77 K.

Fig. 6   Forward-biased I-V characteristics of samples A and B measured at RT or 77 K.

The inset shows the logarithmic I-V plot measured at RT for sample B.

	p^+-Si (200nm)
p^+-Si (200nm)	p-Si (500nm)
p-Si (500nm)	p-β-FeSi$_2$ (90nm)
p-β-FeSi$_2$(90nm)	p-Si (200nm)
n^+-Si(111) Sub.	n^+-Si(111)

(a) Sample A   (b) Sample B
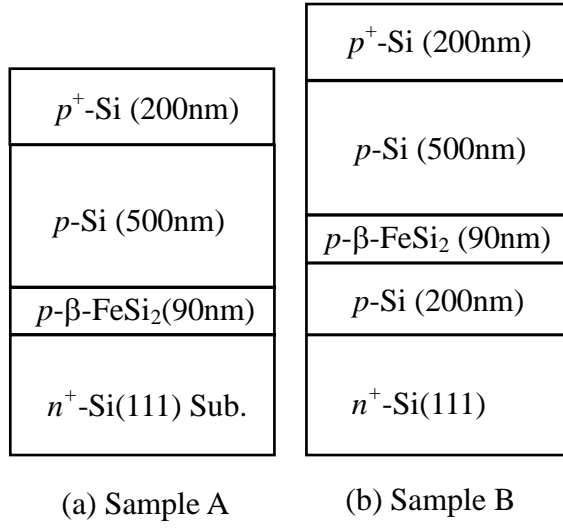
Figure 1　Ugajin *et al*.
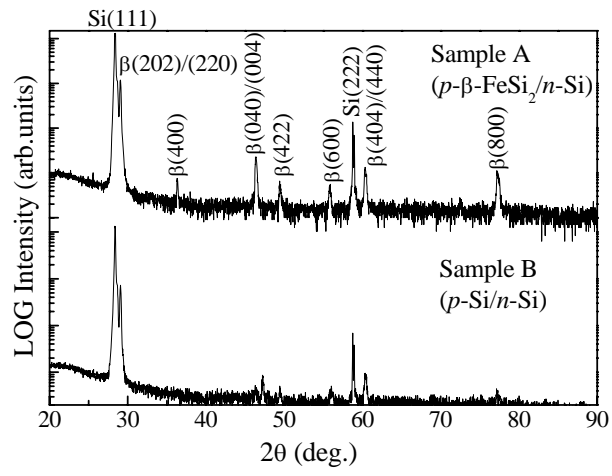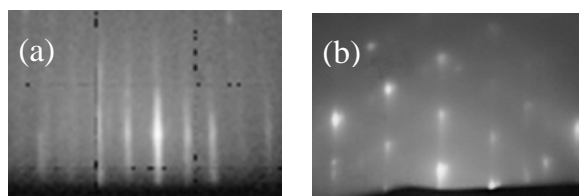
Figure 2   Ugajin *et al*.
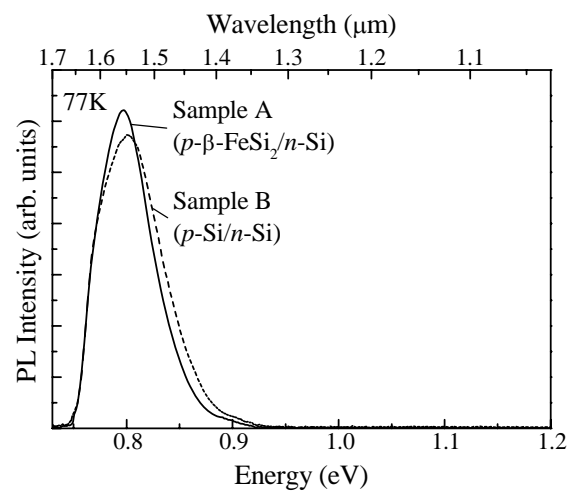
(a)
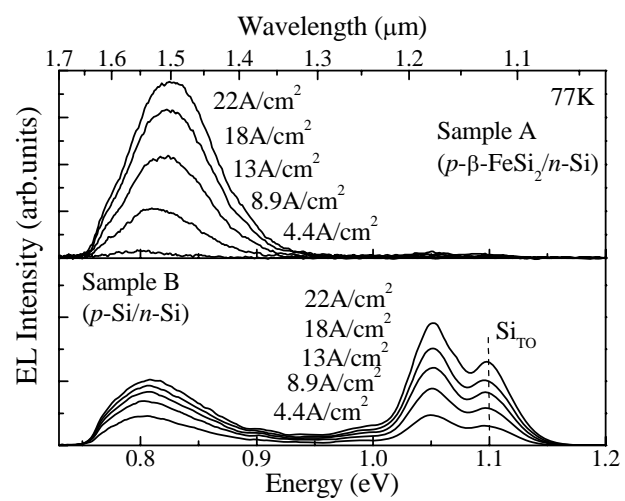
(b)

Figure 3   Ugajin *et al*.

Figure 4   Ugajin *et al*.
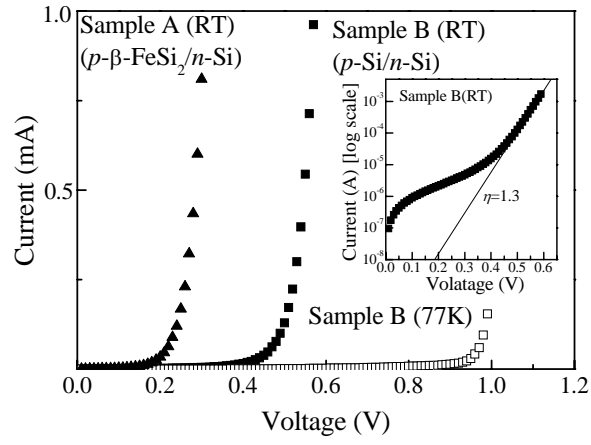
Fig.5　Ugajin *et al.*

Fig.6   Ugajin *et al.*